Chaotic dynamics dependence on doping density in weakly coupled GaAs/AlAs superlattices*

Yang Gui(杨癸)[1, 2, †], Li Yuanhong(李远红)[3], Zhang Fengying(张凤英)[1], and Li Yuqi(李玉琦)[4]

[1]College of Physics & Electrical Engineering, Anyang Normal University, Anyang 455000, China
[2]School of Physics and Electronics, Henan, University, Kaifeng 475004, China
[3]Department of General Education, Henan Vocational College of Chemical Technology, Zhengzhou 450002, China
[4]Henan Institute of Science and Technology, Xinxiang 453003, China

Abstract: A discrete sequential tunneling model is used for studying the influence of the doping density on the dynamical behaviors in weakly coupled GaAs/AlAs superlattices. Driven by the DC bias, the system exhibits self-sustained current oscillations induced by the period motion of the unstable electric field domain, and an electrical hysteresis in the loop of current density voltage curve is deduced. It is found that the hysteresis range strongly depends on the doping density, and the width of the hysteresis loop increases with increasing the doping density. By adding an external driving ac voltage, more complicated nonlinear behaviors are observed including quasi-periodicity, period-3, and the route of an inverse period-doubling to chaos when the driving frequency changes.

Key words: weakly-coupled superlattice; current oscillation; the hysteresis loop
DOI: 10.1088/1674-4926/33/9/092002 **EEACC:** 2520

1. Introduction

Over the last few years, electron vertical transport in superlattices (SLs) has been attracting growing interest and has seen great theoretical[1−8] and experimental[9−11] progress. A variety of new electronic devices can be created based on the study of the novel physical properties of SLs[12−14]. The main electron transport mechanism in weakly coupled n-doped semiconductor SLs is dominated by sequential resonant tunneling between adjacent quantum wells. This has been shown to exhibit a rich variety of strongly nonlinear behaviors[2−6, 15−18] driven by external fields. Owing to the formation of the electric-field domain in SLs, the system shows two different states: one is self-sustained current oscillations (SSCOs) due to the periodic motion of electric field pulse, and the other is a sawtooth-like current–voltage characteristic with many branches associated with static electric field domains (EFDs) when an electric field F is applied along the SL. This is attributed to the pronounced negative differential velocity (NDV) in the electron drift velocity $v_{\rm d}$ versus F characteristic, which is always related to the transport instability. Controlled by the external magnetic fields and the sample temperature, etc[17−19], the NDV curve changes. Consequently, SSCOs are induced in weakly coupled SLs only with appropriate doping and biasing, i.e. in a certain range of the doping level $N_{\rm D}$ and the bias voltage $U_{\rm dc}$[2, 17, 19]. Outside this range, a buildup of stable EFDs for higher carrier concentrations, or a state of almost uniform electric field distribution at lower carrier concentrations, exists[17]. As the AC-voltage is applied, the system shows different complex dynamical behaviors including the period, frequency-locking, quasi-periodicity, and chaos due to strong mixing of internal current oscillations in SLs and the external ac signal.

In this paper, we focus on the hysteresis loop change in the dynamical current density–voltage (J–U) curve, which strongly depends on the doping density. The electron drift velocity is plotted as a function of the electric field. It exhibits NDV which means that the SL is a nonlinear system, and interesting dynamical features can be found. As expected, a hysteresis region exists, which depends on the doping density, becoming wider as the latter increases. For different initial values of SLs in the hysteresis region, the states switch from oscillatary to stationary. Finally, an ac voltage is used to drive the system which exhibits different oscillation modes shown by the phase diagram and corresponding Poincaré maps.

2. The model

Consider a system consisting of N quantum wells driven by a bias voltage perpendicular to the layers. The tunneling electron drift velocity $v_{m\to m+1}$ from well m to well $m+1$ only depends on the electric field F_m. The calculated normalized electron drift velocity as a function of the electric field is depicted in Fig. 1. Clearly, the curve of velocity $v_{\rm d}(F)$ has a maximum corresponding to the occurrence of the electron resonant tunneling, and the region from $F = 1$ to $F = 1.31$ exhibits NDV.

The dynamics of SLs is governed by the following discrete Poisson equations,

$$\frac{1}{l}(F_m - F_{m-1}) = \frac{e}{\varepsilon}(n_m - N_{\rm D}), \tag{1}$$

$$\varepsilon(F_m - F_0)/(el) = n_1 - N_{\rm D} = \delta N_{\rm D}, \tag{2}$$

* Project supported by the National Natural Science Foundation of China (Nos. 11047108, 11147197, 11005003), the Research Project of Basic and Cutting-Edge Technology of Henan Province, China (No. 112300410183), and the Education Department of Henan Province, China (No. 2011B140002).

† Corresponding author. Email: kuiziyang@126.com

Received 7 March 2012, revised manuscript received 23 May 2012

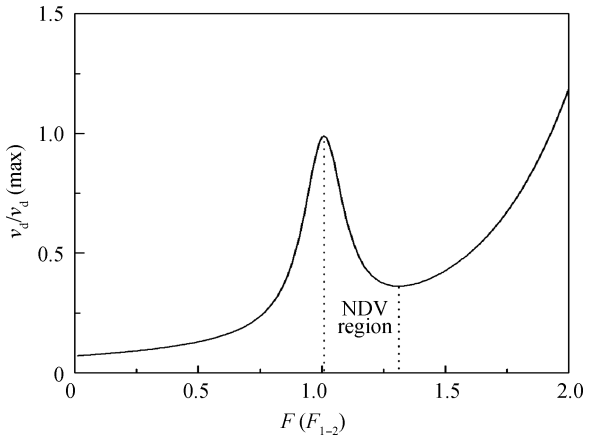

Fig. 1. Normalized electron drift velocity $v_{\rm d}$ as a function of the electric field.

and the current continuity equation, the applied voltage bias conditions between the emitter and collector:

$$\varepsilon\frac{{\rm d}F_m}{{\rm d}t} + e n_m v_{\rm d}(F_m) = J(t), \tag{3}$$

$$l\sum_{i=1}^{N} F_m = U(t). \tag{4}$$

In the spatially homogeneous case, the value of n_m and n_{m+1} is equal to the doping density $N_{\rm D}$, i.e. $n_m = n_{m+1} = N_{\rm D}$. Equation (2) is the boundary condition with δ as a model parameter. Here $m = 1, 2, \ldots, N$ is the well index, F_0, $F_{\rm N}$ correspond to the electric fields at the emitter and collector, and ε and e are the permittivity and electron charge, respectively. The total current density $J(t)$ is the sum of the displacement current and the electron flux via a series of sequential resonant tunnelings. The total applied voltage $U(t)$ in Eq. (4) can be written as $U(t) = U_{\rm dc}[1 + A\sin(2\pi f_{\rm d}t)]$ with $U_{\rm dc}$ is the DC voltage, A and $f_{\rm d}$ are the relative amplitude and driving frequency of an ac bias signal.

To make a convenient calculation, the variables are dimensionalized as follows:

$\Phi_m = F_m/F_{1-2}$, $F_{1-2} = (E_2 - E_1)/(el)$, $n_0 = \varepsilon F_{1-2}/(el)$, $\lambda = N_{\rm D}/n_0$, $t_{\rm tun} = l/v_{\rm d}(F_{1-2})$, $\tau = t/t_{\rm tun}$, $w = 2\pi f_{\rm d}t_{\rm tun}$, $V = U_{\rm dc}/(F_{1-2}lN)$ and $a = AV$.

Combining Eqs. (1)–(4), we obtain N dimensionless equations for the electric field.

$$\frac{{\rm d}\Phi_m}{{\rm d}\tau} = \frac{1}{N}\sum_{j=1}^{N} v_{\rm d}(\Phi_n)[\Phi_n - \Phi_{n-1} + \lambda] - v_{\rm d}(\Phi_n) \times [\Phi_m - \Phi_{m-1} + \lambda] + aw\cos(w\tau). \tag{5}$$

Equation (5) can be solved by the fourth-order Runge-Kutta method.

3. The hysteresis loop in the dynamical current density–voltage curve

We simulate numerically an $N = 30$ weakly GaAs/AlAs (n-doped/undoped) SL with a $w = 9.0$ nm GaAs well and $d = 4.0$ nm AlAs barriers, i.e. the period of the SL $l = 13.0$ nm. The difference between the first excited state and the ground state is $\Delta = E_2 - E_1 = 135$ meV. The lattice temperature is fixed at $T = 20$ K, and the value $\delta = 0.001$.

Following the initial transient behavior, the current density $J(t)$ either reaches a constant value or oscillates between minima $J_{\rm min}$ and maxima $J_{\rm max}$, which depend on the bias $U_{\rm dc}$ and the doping density λ. Figures 2(a)–2(d) show the $J(U)$ curves calculated at different doping densities $\lambda = 0.045$, 0.065, 0.085, and 0.105. For all λ, each trace is single-valued at low $U_{\rm dc}$ and the stationary behavior occurs. But when $U_{\rm dc}$ exceeds a critical value $U_{\rm c}$, which depends on λ, the stationary state loses its stability via Hopf bifurcation and $J(t)$ starts to oscillate corresponding to multiple values in the shaded regions. The states of the system will be transformed between static and dynamic at the left, U_{ci} (i = a, b, c, and d), and right, U_{ij} ($j = 1, 2$), bifurcation point, denoted by the arrow in Fig. 2. In contrast with the upper and lower figures in Figs. 2(a)–2(d), respectively, the corresponding value $U_{\rm ci}$ is associated with the left bifurcation point. However, the value of the right bifurcation point corresponding to the applied voltage U_{ij} is different, which indicates that the hysteresis loop is produced in the dynamical current density–voltage (J–U) curve.

Now, we consider in detail how the width of the hysteresis loop varies with different doping densities. For $\lambda = 0.045$, $J(t)$ starts to exhibit periodic oscillations up to $U_{\rm ca} = 31.404$. When the control parameter increases to $U_{\rm a1} = 35.078$, the oscillation disappears and the system transforms to a stable equilibrium state. On the other hand, with a decrease of the control parameter $U_{\rm dc}$, the oscillation does not occur until $U_{\rm a2} = 34.790$. Comparing with the change in voltage, this means that the hysteresis loop exists and its range is $U_{\rm a1} - U_{\rm a2} = 0.288$. The J–U curves calculated for $\lambda = 0.065$, $\lambda = 0.085$, and $\lambda = 0.105$, are very similar to those for $\lambda = 0.045$ (Fig. 2(a)). The corresponding ranges of the hysteresis loop are $U_{\rm b1} - U_{\rm b2} = 1.055$, $U_{\rm c1} - U_{\rm c2} = 2.905$, and $U_{\rm d1} - U_{\rm d2} = 5.250$. Hence, the range of the hysteresis loop changes with doping density, becoming wider for a higher doping concentration. If the applied voltage is set in the hysteresis range and takes different initial values, the nonlinear system can evolve into different types of attractor: a zero-dimensional attractor of a fixed point or a one-dimensional attractor of a limit cycle.

4. Chaotic dynamics due to the frequency coupled between the internal oscillations and external ac signals

In this section, the dynamics of the system is investigated by varying the dc and ac voltage, i.e. the applied voltage can be written as $U(t) = U_{\rm dc}[1 + A\sin(2\pi f_{\rm d}t)]$. An inherent feature of periodically forced nonlinear systems is that the actual oscillation frequency depends on the amplitude of the forcing. Therefore both the frequency $f_{\rm d}$ and the amplitude A of the driving can be used as control parameters to study nonlinear dynamics. The dc voltage is chosen as $U_{\rm dc} = 35.7$ V, and the doping density $\lambda = 0.05$. The relative amplitude is fixed at $a = 0.08$, and the driving frequency $0 < f_{\rm d}/f_0 < 2.4$, where $f_0 = 0.0122/t_{\rm tun}$ is the natural current oscillation frequency. Such a choice is sufficient to describe the interesting nonlinear

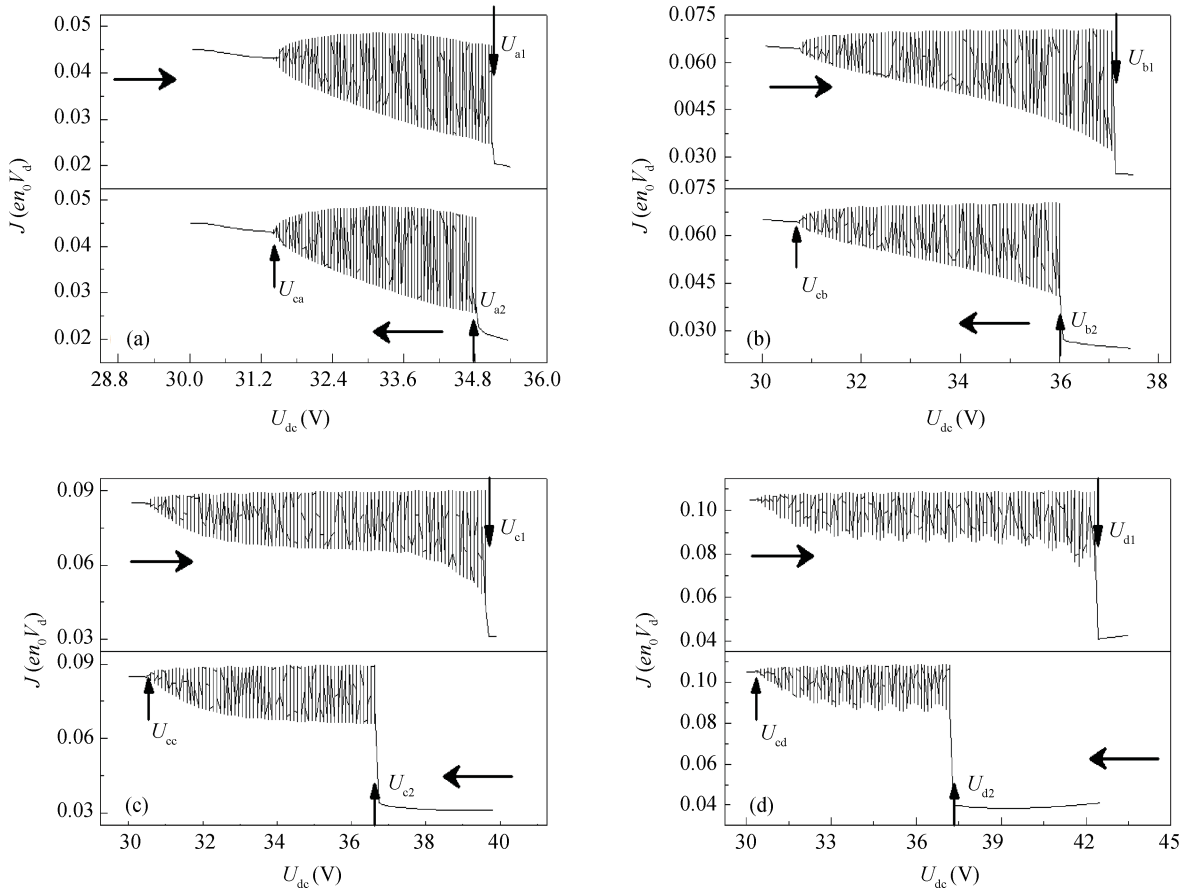

Fig. 2. Hysteresis loops in the current density–voltage (J–U) curve for different doping densities. (a) $\lambda = 0.045$. (b) $\lambda = 0.065$. (c) $\lambda = 0.085$. (d) $\lambda = 0.105$.

dynamical behaviors.

The Poincaré map in the current density versus the driving frequency f_d/f_0 space is used to study the dynamics of the system. Let $T_d = 1/f_d$ be the driving period and sample the current density J_n at times $T_n = nT_d$, $n = 1, 2, \ldots$ (after waiting enough time for the transients to have decayed). For each f_d, we calculate $J_n = J(nT_d)$ until the solution becomes stable within a 10^{-5} accuracy. At that time, stop the simulation and record all the J_n corresponding to one period of the solution. Thus, the Poincaré map is obtained with the change in driving frequency as shown in Fig. 3. The oscillation modes can be estimated by the number of points in the Poincaré bifurcation diagram. For a period-n solution, they appear as simple closed loops in the phase diagram, and n separate points in the Poincaré map. But for chaos, the phase diagram and the Poincaré return map will be more complicated. From Fig. 3, the system displays a period-1 oscillation which corresponds to one point in the Poincaré map at the beginning of $0 < f_d/f_0 < 0.763$. With a further increase of the driving frequency to $0.763 \leqslant f_d/f_0 < 2.075$, the system displays different nonlinear dynamics such as period-n and chaos. The phase portraits and corresponding Poincaré map for period-2, period-4, chaos and period-3 are plotted in Figs. 4(a)–4(d) with different driving frequencies: $f_d/f_0 = 0.793$, 1.188, 1.42, and 1.81, respectively. In the case of $2.075 \leqslant f_d/f_0 < 2.4$, the route of an inverse period-doubling to chaos is deduced. The corresponding dynamical behaviors are shown in Figs. 5(a)–5(d) for

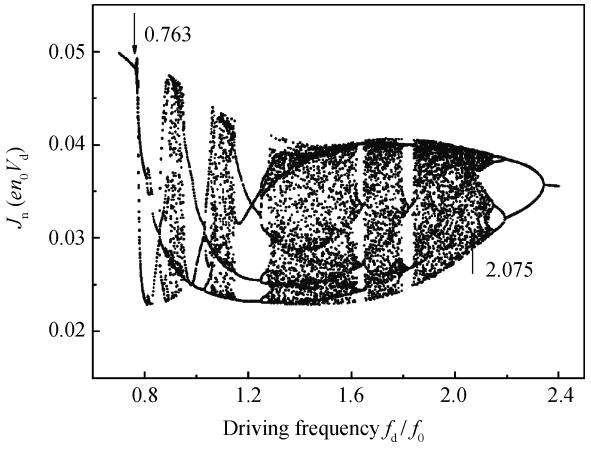

Fig. 3. A Poincaré bifurcation diagram of the current density J_n versus the driving frequency $0 < f_d/f_0 < 2.4$ with the doping density $\lambda = 0.05$.

driving frequencies of $f_d/f_0 = 2.273$, 2.164, 2.135, and 2.081, respectively.

5. Conclusions

The dynamics of a traveling electric field domain in a biased weakly coupled SL can be controlled by the doping density λ. In the dynamical current density versus voltage (J–U)

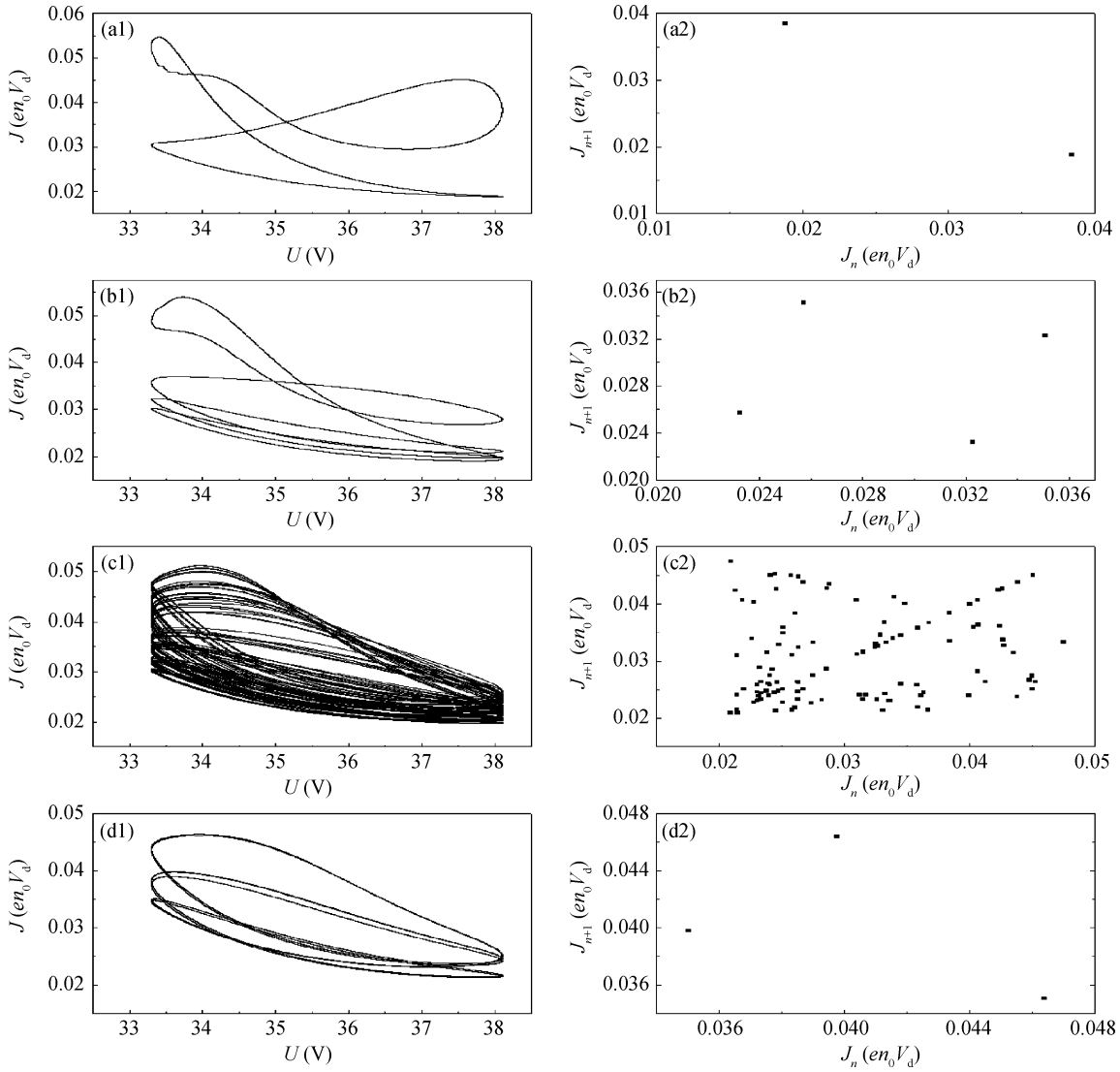

Fig. 4. Phase portraits (left) and the corresponding Poincaré map (right) for different frequencies. (a) $f_d/f_0 = 0.793$ (period-2). (b) $f_d/f_0 = 1.188$ (period-4). (c) $f_d/f_0 = 1.42$ (chaos). (d) $f_d/f_0 = 1.81$ (period-3).

curve, a hysteresis loop occurs, whose range is affected by the doping density. For a value $\lambda = 0.045$, the hysteresis range exists but its range $U_{a1} - U_{a2} = 0.288$ is not obvious. With a further increase of λ to 0.065, 0.085, and 0.105, the hysteresis range increases to $U_{b1} - U_{b2} = 1.055$, $U_{c1} - U_{c2} = 2.905$, and $U_{d1} - U_{d2} = 5.250$, respectively. In addition, an ac voltage is applied to drive the SL and it exhibits complex dynamical behaviors due to frequency coupled between the internal current oscillations and the external ac signal. A Poincaré bifurcation diagram is plotted to detect the oscillation modes such as frequency-locking, quasi-periodicity, period and chaos.

References

[1] Esaki L, Chang L L. New transport phenomenon in a semiconductor superlattice. Phys Rev Lett, 1974, 33: 495

[2] Bulashenko O M, García M J, Bonilla L L. Chaotic dynamics of electric-field domains in periodically driven superlattices. Phys Rev B, 1996, 53: 10008

[3] Bonilla L L, Escobedo R, Dell'Acqua G. Voltage switching and domain relocation in semiconductor superlattices. Phys Rev B, 2006, 73: 115341

[4] Dreisow F, Szameit A, Heinrich M, et al. Bloch-Zener oscillations in binary superlattices. Phys Rev Lett, 2009,102: 076802

[5] Romanov Y A, Romanova J Y, Mourokh L G. Electron Bloch oscillations and electromagnetic transparency of semiconductor superlattices in multi-frequency electric fields. Phys Rev B, 2009, 79: 245320

[6] Escobedo R, Carretero M, Bonilla L L, et al. Self-sustained spin-polarized current oscillations in multiquantum well structures. New J Phys, 2009, 11: 013033

[7] Luo Shiyu, Shao Mingzhu. Small amplitude approximation and dynamic stabilities of a strained superlattice. Chinese Journal of Semiconductors, 2005, 11: 2097

[8] Deng Chengliang, Luo Shiyu, Shao Mingzhu. Sine-squared potential and chaotic behaviour of strained superlattice. Chinese Journal of Semiconductors, 2005, 11(2): 294

[9] Sun B Q, Wang J N, Ge W K, et al. Current self-oscillation induced by a transverse magnetic field in a doped GaAs/AlAs superlattice. Phys Rev B, 1999, 60: 8866

[10] Sun Z Z, Sun Y, Wang X R, et al. Self-sustained current oscillations in superlattices and the van der Pol equation. Appl Phys

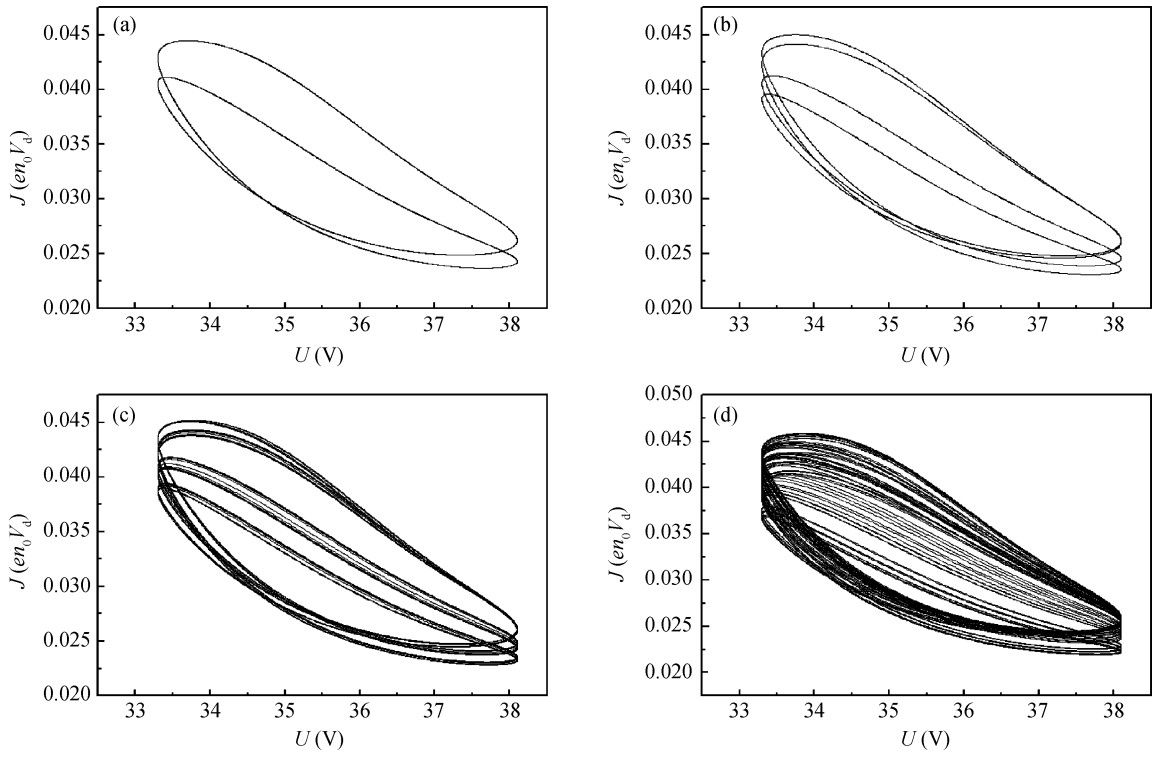

Fig. 5. An inverse route from period-doubling to chaos with the change of different driving frequencies. (a) $f_d/f_0 = 2.273$ (period-2). (b) $f_d/f_0 = 2.164$ (period-4). (c) $f_d/f_0 = 2.135$ (period-8). (d) $f_d/f_0 = 2.081$ (chaos).

Lett, 2005, 87: 182110

[11] Lhuillier E, Ribet-Mohamed I, Nedelcu A, et al. Quantum transport in weakly coupled superlattices at low temperature. Phys Rev B, 2010, 81: 155305

[12] Hyart T, Alekseev K N, Thuneberg E V. Bloch gain in dc-ac-driven semiconductor superlattices in the absence of electric domains. Phys Rev B, 2008, 77: 165330

[13] Savvidis P G, Kolasa B, Lee G, et al. Resonant crossover of terahertz loss to the gain of a bloch oscillating InAs/AlSb superlattice. Phys Rev Lett, 2004, 92: 196802

[14] Bao M, Wang K L. Accurately measuring current–voltage characteristics of tunnel diodes. IEEE Trans Electron Devices, 2006, 53: 2564

[15] Yang G, Zhao H W, Meng H, et al. The dynamics of GaAs/AlGaAs heterostructure under the transverse magnetic fields and microwave irradiations. Int J Mod Phys B, 2009, 23(15): 3305

[16] Arana J I, Bonilla L L, Grahn H T. Photoexcited semiconductor superlattices as constrained excitable media: motion of dipole domains and current self-oscillations. Phys Rev B, 2010, 81: 035322

[17] Yang G, Meng H, Zhang L F, et al. The self-sustained current oscillation and the dynamics in superlattices under the action of electric and magnetic fields. J Appl Phys, 2008, 103: 123701

[18] Wang C, Cao J C. Current oscillation and chaotic dynamics in superlattices driven by crossed electric and magnetic fields. Chaos, 2005, 15: 013111

[19] Sun Z Z, Chen K L, Yin S, et al. Transcritical Hopf bifurcation and breathing of limit cycles in sequential tunnelling of superlattices. New J Phys, 2004, 6: 148